



3-1-7

### SIMULATION ANALYSIS FOR THE TIME-SPACE VARIATION WITHIN THE LOCAL SEISMIC ARRAY

Kenichi KATO<sup>1</sup>, Masamitsu MIYAMURA<sup>1</sup>, Shizuo NODA<sup>2</sup>, Tokiharu OHTA<sup>3</sup>

<sup>1</sup>Kobori Research Complex, Kajima Corporation,  
Shinjuku-ku, Tokyo, Japan

<sup>2</sup>The Tokyo Electric Power Company,  
Chiyoda-ku, Tokyo, Japan

<sup>3</sup>Kajima Institute of Construction Technology,  
Choufu-city, Tokyo, Japan

#### SUMMARY

It is important to study the characteristics of the time-space variations of ground motions for the evaluation of the realistic input ground motion to large scale structures. The geographical features surrounding observation points are modeled and analyzed by Boundary Element Method in order to study the effect of local topography and incident angle of ground motions. The results indicate that the observed horizontal phase lags in the frequency range lower than about 2Hz correspond to the BEM results with a 15° incident angle, while the phase lags in higher frequency components are influenced more by local topography than incident angle. A simulation analysis of closely-spaced ground motions is attempted here based on the BEM results.

#### OUTLINE OF THE OBSERVATION SYSTEM AND SUMMARY OF THE OBSERVED GROUND MOTIONS

An accurate earthquake instrument array has been placed in operation since December 1978 at four separate rock sites surrounding Tokyo within radius of 150 km (Ref.1). At one of the four array networks, the Higashimatuyama station, six observation points(No.2,3,4,5,7,8) are placed on relatively hard rock with a shear wave velocity  $V_s$  of 700-800 m/sec and geological period of Miocene in Tertiary. Fig.1 shows the arrangement of the observation system.

Until present time, numerous ground motion records have been obtained. One of the largest earthquakes recorded by the array (February 12, 1984) is selected in this paper. The outline of the earthquake and epicenter are shown in Table 1 and Fig.2.

#### ANALYSES OF OBSERVED GROUND MOTIONS

Variation of Frequency Content of Adjacent Ground Motions In order to investigate the variation of frequency content for 6 horizontally separated observation points, power spectra for 5 seconds of S waves are calculated and smoothed by using Hanning type window as shown in Fig.3. The shapes of smoothed power spectra of No.3, No.5, No.8 observation points show peculiar peaks from 2.0 to 4.0Hz, while those of No.2, No.4, No.7 show less significant peaks and the spectral shapes seem to be similar. This tendency suggests that the frequency content changes even within a radius of 500m. For the quantitative evaluation of these variations, coherence functions are computed for the two pairs of observation points, No.2-4 and No.2-8 of which distances are 417m and 370m

respectively. The direction of an epicenter is on the straight line from No.4 to No.8. Fig.4 shows the comparison of coherence functions for No.2-4 and No.2-8. The coherence functions show higher values and similar characteristics in the frequency range lower than around 1Hz.

Variation of Phase Lags of Adjacent Ground Motions In order to investigate the variation of phase lags for horizontally separated two observation points, circular phase spectra were defined(Ref.2,3) and computed. Fig.5 shows the phase spectra of No.2-8 and No.2-4 from 0 to 5Hz for 5 seconds of S waves. The phase lags up to around 2Hz show the specific feature which implies that the non-vertical wave propagates horizontally from the No.8 to the No.4 observation point. On the other hand, the phase lags over 2Hz indicate a large variance. This variance is assumed to be caused by local topography surrounding the observation points.

#### ANALYSES OF LOCAL TOPOGRAPHY BY BOUNDARY ELEMENT METHOD

Idealization of Local Topography Based on the detailed investigation results of soil profile, Boundary Element Method(BEM) is applied for the study of the effect of local topography and incident angle. Fig.6 shows the soil profile along the section of No.2-4. The depth of surface layer is about 50m and its shear wave velocity  $V_s$  ranges from 0.3 to 0.7Km/sec. Local topography is idealized into two parts with constant physical parameters, the first being a surface layer and the second being a semi-infinite medium. Fig.7 and Table 2 shows the idealized model and soil properties. Based on the idealized model, response analyses are carried out in frequency domain from 0 to 5 Hz by changing the incident angles from  $0^\circ$  to  $15^\circ$  for the SH and SV waves.

Study of the Phase Lags of Adjacent Ground Motions The phase lags of No.4 and No.8 to No.2 are calculated. Fig.8 shows the results of SH wave analysis. White circles shown in the case of  $15^\circ$  incident angle indicate the observed phase lags. The results indicate that observed phase lags in the frequency range lower than around 2Hz approximately correspond to the BEM results. On the other hand, the phase lags in the frequency range higher than 2Hz show a relatively large variance implying that the influence of local topography is significant. This tendency can be seen especially in case of incident angle  $0^\circ$ . Fig.9 shows the results of SV wave analysis. The similar tendency can be seen as that of SH waves.

Study of the Spectral Ratio of Adjacent Ground Motions The spectral ratios of No.4 and No.8 to No.2 are calculated. Fig.10 shows the results of SH wave analysis, and observed spectral ratio is shown by solid line for the comparison. The value of analytical spectral ratio is nearly 1.0 in the frequency range lower than around 2Hz, while it shows a variance in the frequency range higher than 2Hz. Fig.11 shows the result of SV waves. Though the analytical results of SH and SV waves show similar tendency as a whole, the difference between the analytical and observed results is relatively large in high frequency range, especially in the case of No.8/No.2

#### SIMULATION OF CLOSELY-SPACED GROUND MOTIONS

Proposal of Frequency-dependent Superposition Method A developed simulation method is proposed based on the results of BEM analysis in order to simulate the closely-spaced ground motions. As an example case, the ground motions of No.4 and No.8 are simulated by making use of observed No.2 wave. According to the BEM results, frequency components lower than around 2Hz are governed by the incident angle, while higher frequency components are influenced by local topography. Therefore, simulation process is divided into two steps as shown in Fig.12. In the frequency range lower than 2Hz, the amplitudes of ground motions of No.4 and No.8

are assumed to be equal to that of No.2 and the phase lags are modified in accordance with the wave propagation path based on the incident angle. In the frequency range higher than 2Hz, the amplitudes of ground motions are modified by the spectral ratio which was obtained from BEM analysis. Here, the phase lags are given as random number because the phase lags do not show specific features in this frequency range from the analyses of observed waves. Considering the changes of the amplitude and phase lags in each frequency component, simulation waves are generated by the superposition of time histories defined by two frequency bands.

Comparison of Observed and Simulated Waves As a comparison of time histories, Fig.13 shows an example of simulated wave of No.4 derived from No.2 in the frequency range lower than 2Hz. The simulated wave seems to represent the form of observed wave. As the second step, smoothed power spectra of observed and simulated wave are computed and shown as Fig.14 in order to compare the frequency content. The frequency content of both waves approximately corresponds to each other.

#### CONCLUSIONS

From these analyses, the following can be concluded:

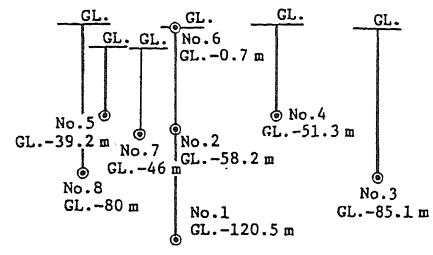
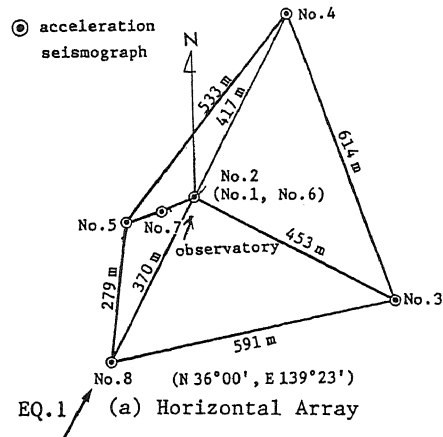
- (1) The observed phase lags between measuring points within the distance of 400m correspond to the BEM results with 15° incident angle in the frequency range lower than 2 Hz.
- (2) The phase lags are influenced by local topography surrounding the observation points in the frequency range higher than 2Hz.
- (3) These analyses are carried out assuming stationary process. However, time-dependent characteristics of frequency components and phase lags are significant in several observed waves. Therefore, non-stationary process should be taken into consideration in future analysis.

#### ACKNOWLEDGMENT

We are grateful to Mr. K. Takahashi, H. Koshida, S. Hiehata in Kajima Corporation who provided us with valuable comments and advice, and also are thankful to Mr. N. Kurata who helped the computation in this study. Valuable earthquake data were offered by "Committee of Strong-Motion Instruments Array" (Chairman is Prof. S. Omote).

#### REFERENCES

1. S. Omote, et al. "Recent Developed Strong Motion Earthquake Instruments Array in Japan" 7WCEE INSTANBUL 1980.
2. K. Muto, et al. "Analysis of Strong Ground Motions Observed in Earthquake Instruments Array" 8WCEE SAN FRANCISCO 1984.
3. M. Miyamura, et al. "Time-dependent Variation of Ground Motions Observed at Local Seismic Array" 8th European Conference on Earthquake Engineering Lisbon 1986.
4. M. Hoshiya, et al. "Simulation of Spatially and Temporally Variative Earthquake Ground Motions" Proc. of JSCE No.386/I-8 1987-10.
5. Ronald S. Harichandran and Erik H. Vanmarcke "Stochastic Variation of Earthquake Ground Motion in Space and Time" Journal of Engineering Mechanics Division Vol.112 No.2 1986.2.



(b) Vertical Array  
Fig.1 Plan of observation Points

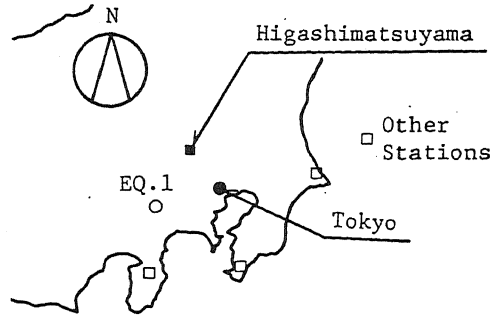


Fig.2 Epicenter of the Earthquake

Table 1 Outline of the Earthquake

EQ.No.	DATE	M	$\Delta$ (km)	h(km)
EQ.1	1984 2.14	5.2	52	25

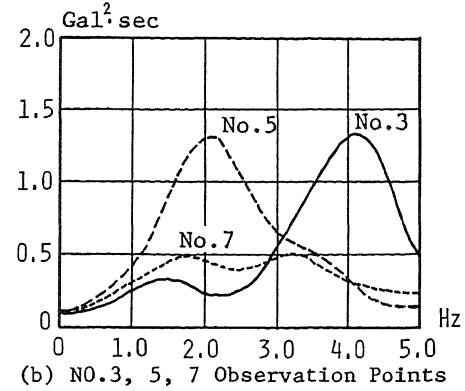
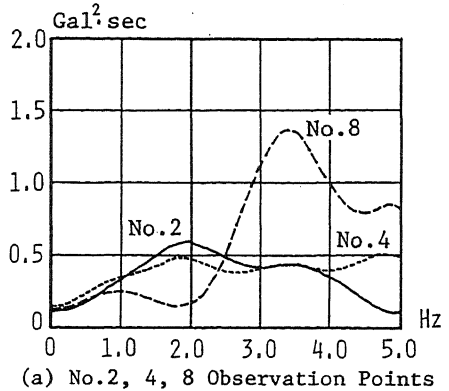


Fig.3 Comparison of Smoothed Power Spectra (T - Direction)

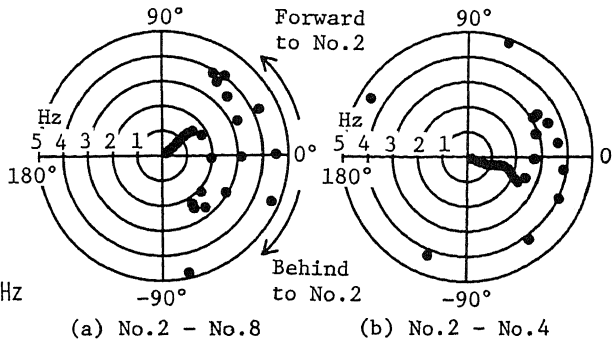
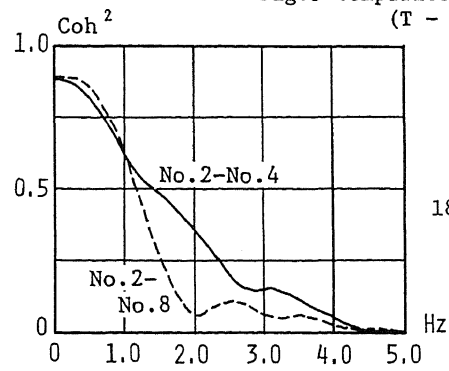


Fig.4 Comparison of Coherence between No.2 and No.4, No.8 (T - Direction)

Fig.5 Circular Phase Spectra Obtained by Observed Waves (T - Direction)

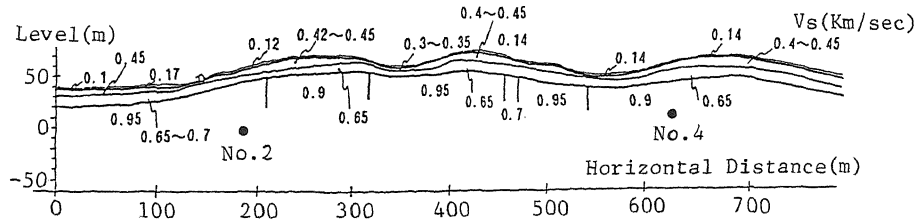
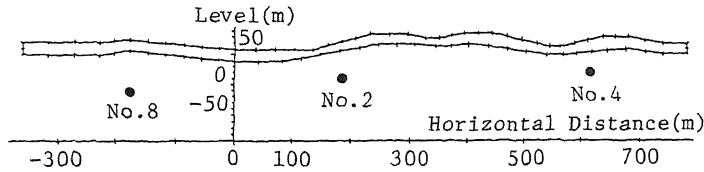


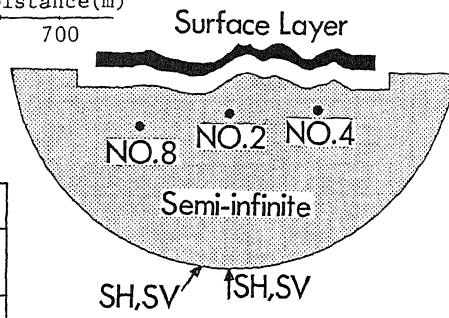
Fig.6 Soil Profile from No.2 to No.4



(a) Model for Surface Layer

Table 2 Material Properties of Soil

	Vs(m/sec)	$\rho$ (g/cm <sup>3</sup> )	$\mu$
Surface Layer	500	1.5	0.40
Semi-infinite Medium	900	2.0	0.42



(b) Model for Semi-infinite Medium

Fig.7 BEM Model of Local Topography

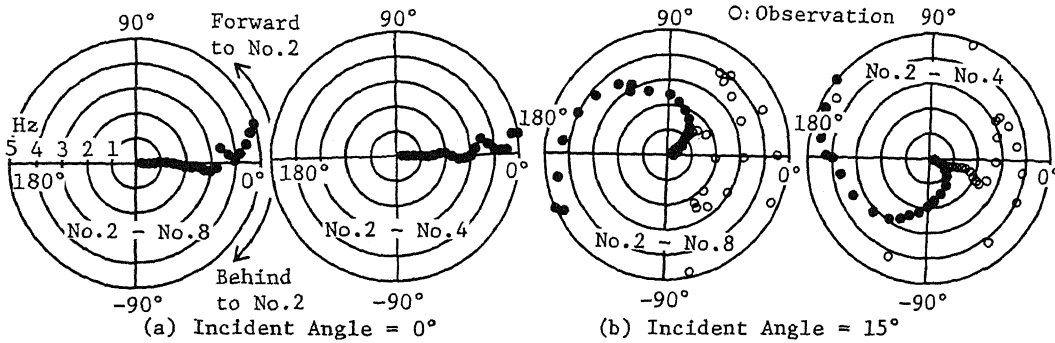


Fig.8 Circular Phase Spectra Based on BEM Analysis (SH Wave)

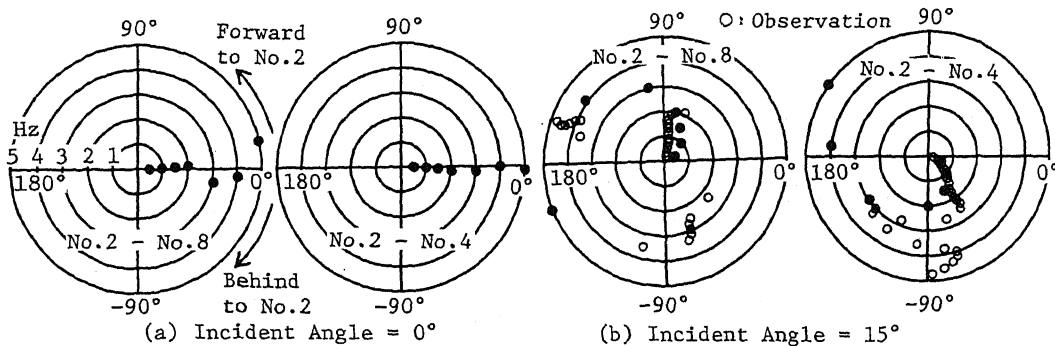


Fig.9 Circular Phase Spectra Based on BEM Analysis (SV Wave)

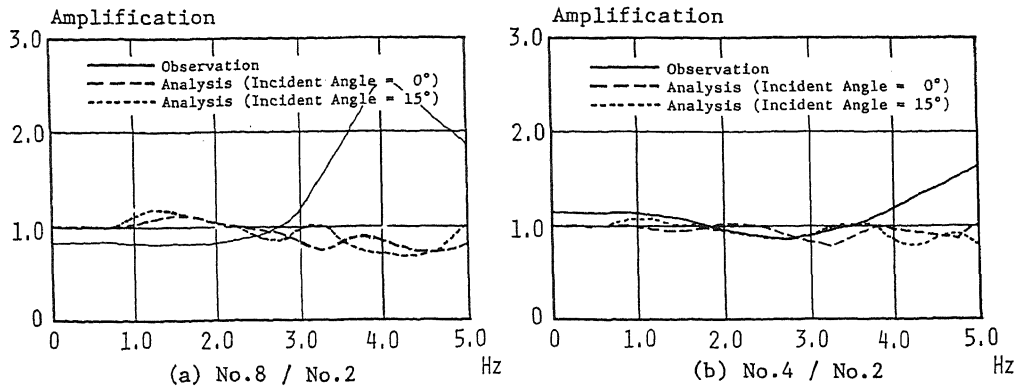


Fig.10 Spectral Ratios Based on BEM Analysis (SH Wave)

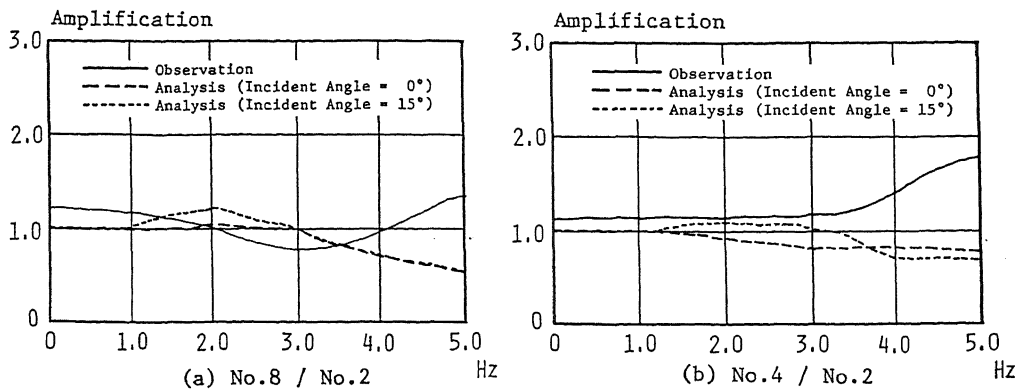


Fig.11 Spectral Ratios Based on BEM Analysis (SV Wave)

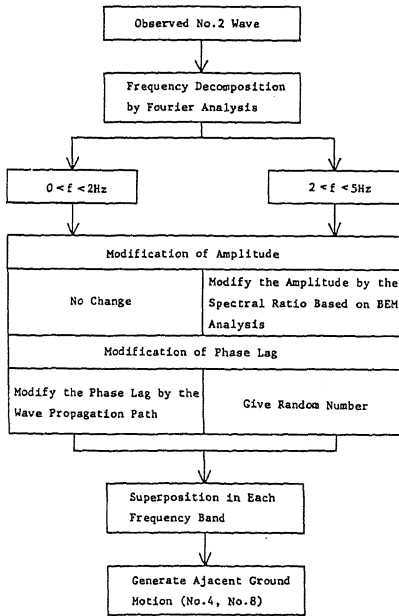


Fig.12 Flow Chart for Simulation of Adjacent Ground Motion

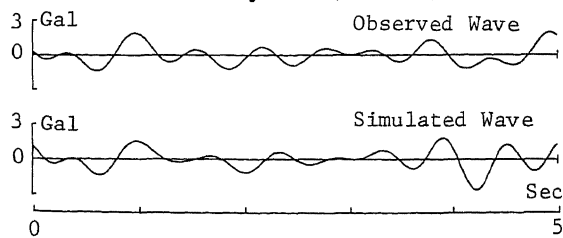


Fig.13 Comparison of Observed and Simulated Ground Motions (No.4 T-Direction, 0.2-2.0Hz)

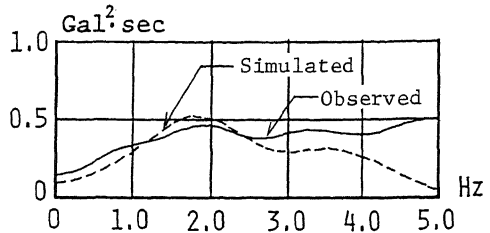


Fig.14 Comparison of Observed and Simulated Power Spectra (No.4 T-Direction)